Redshift and redshift drift in $\Lambda = 0$ quasispherical Szekeres cosmological models and the effect of averaging

Priti Mishra*

Department of Physics, Magadh Mahila College, Patna Universirty, North Gandhi Maidan, Patna-800001, Bihar, India

(Received 24 September 2018; accepted 2 March 2022; published 18 March 2022)

Since the advent of the accelerated expanding homogeneous universe model, some other explanations for the type Ia supernova dimming have been explored, among which there are inhomogeneous models constructed with exact $\Lambda = 0$ solutions of Einstein's equations. They have been used either to be a one patch or to build Swiss-cheese models. The most studied ones have been the Lemaître-Tolman-Bondi (LTB) models. However, these models being spatially spherical, they are not well designed to reproduce the large scale structures which exhibit clusters, filaments, and nonspherical voids. This is the reason why Szekeres models, which are devoid of any symmetry, have recently come into play. In this paper, we give the equations and an algorithm to compute the redshift drift for the most general quasispherical Szekeres (QSS) models with no dark energy. We apply it to a QSS model recently proposed by Bolejko and Sussman (BSQSS model) who averaged their model to reproduce the density distribution of the Alexander and collaborators' LTB model which is able to fit a large set of cosmological data without dark energy. They concluded that their model represents a significant improvement over the observed cosmic structure description by spherical LTB models. We show here that this QSS model is ruled out by a negative cosmological redshift, i.e., a blueshift, which is not observed in the universe. We also compute a positive redshift and the redshift drift for the model of Alexander *et al.* and compare this redshift drift to that of the ΛCDM model. We conclude that the process of averaging an unphysical QSS model can lead to obtain a physical model able to reproduce our observed local universe with no dark energy need and that the redshift drift can discriminate between this model and the ΛCDM model. For completeness, we also compute the blueshift drift of the BSQSS model.

DOI: 10.1103/PhysRevD.105.063520

I. INTRODUCTION

In 1998 the type Ia supernova (SN Ia) observations revealed that their observed luminosity was lower than what was expected in the cold dark matter (CDM) model [1,2]. In other words, the SN Ia were found to be at a distance farther than that predicted by the CDM model. Also, the deceleration parameter was found to be negative in the CDM model. A negative deceleration parameter implies that the universe expansion rate is accelerating. This can be explained in Friedmann-Lemaître-Robertson-Walker (FLRW) metric models only if a fluid with negative pressure is assumed to fill the universe. Such an exotic fluid is named dark energy. Since this discovery, there have been many dark energy models proposed in the literature, but none of them satisfactorily addresses the question of its origin and nature [3]. There are a number of reported cases where the ΛCDM model cannot explain some observational phenomena, or where the constraint on cosmological parameters coming from different experiments seem to be inconsistent with each other [4,5].

However, there have been attempts to explain these observations without assuming any dark energy component. The main attempts can be broadly divided into two categories: inhomogeneous models and modified gravity. As the names suggest, the first category abandons the space homogeneity assumption and the second category works with modified Einstein's equations (see, e.g., Refs. [6–8], and Ref. [9] for a review). In this article, we limit ourselves to the study of inhomogeneous models.

The two inhomogeneous solutions of Einstein's equations which have been most frequently used in the literature can be divided into two classes: Lemaître-Tolman-Bondi (LTB) [10–12] models and Szekeres [13] models. The LTB metric is a spatially spherical dust solution of the Einstein equations while the Szekeres metric is a dust solution of these equations with no symmetry, i.e., no Killing vector [14]. One can find in the literature many LTB models and a few Szekeres models which claim to explain the cosmological observations without assuming dark energy (see, e.g., Ref. [15] for a review and also Refs. [16–18] for a

*preet.tifr@gmail.com

study of a particular Szekeres model not included in this previous review). Since these solutions are considering only dust as a gravitational source, they are valid only in the universe region where the radiation effect is negligible, i.e., between the last scattering surface and our current location. We will use them to study our local universe where dark energy is supposed to have the strongest effect.

Most spherical LTB void models have been ruled out, but more general nonspherical inhomogeneities still need to be tested by observation [19]. More discriminators should be computed to find out which model of the universe can explain all the cosmological observations. In this paper, we are interested in the study of the Szekeres model proposed by Bolejko and Sussman [20], which, once spatially averaged, reproduces qualitatively the density profile of the LTB model of Alexander and collaborators (A09 model) [21]. This LTB model is a very good fit to the SN Ia data and is also consistent with the WMAP three-year data and local measurements of the Hubble parameter.

However, for models reproducing cosmological data measured on our past light cone, the discrimination between inhomogeneous models and ΛCDM models is impossible. The problem is completely degenerate. This is the reason why several tests using effects outside the light cone have been proposed, one of these being the source redshift drift while the observer's proper time is elapsing [22,23].

In a previous paper [24], we have calculated the redshift drift for the axially symmetric Szekeres model of Ref. [25] and compared it to the redshift drift in some LTB models found in the literature and to that of the ΛCDM model. We found that the redshift drift is indeed able to distinguish between these different models.

Here, our first purpose was to compute the redshift drift for the most general Szekeres model of Bolejko and Sussman which displays no symmetry and for the LTB A09 model to see whether upon averaging the redshift drift changes significantly and then to compare these redshift drifts to that in the ΛCDM model.

We have thus calculated the equations and written a code able to compute, among other features, the redshift and the redshift drift of the most general quasispherical Szekeres (QSS) model. We have applied this code to the Bolejko and Sussman quasispherical Szekeres (BSQSS) model. We have also computed these quantities for the A09 model with the same recipe used in our previous [24] paper. However, we found that the BSQSS model exhibits a negative cosmological redshift, i.e., a blueshift, which is not observed in the universe. This must be considered as enough to rule out the model; however, for completeness, we have computed the blueshift drift for this model.

The structure of the present paper is as follows. In Sec. II, we present the Szekeres models and the particular QSS subclass used here. In Sec. III we display the differential equations for the redshift and the redshift drift in the most general QSS models and an algorithm to numerically integrate them. In Sec. IV we compute the redshift and the redshift drift in the model proposed by Bolejko and Sussman [20]. In Sec. V, we display our results for the redshift and redshift drift computation in the LTB model studied by the A09 model [21]. In Sec. VI, we present our conclusions.

II. SZEKERES MODELS

The Szekeres metric [13] is the most general dust solution of Einstein's equations. By the most general solution we mean that this solution has no symmetry; i.e., it has no Killing vector. In comoving and synchronous coordinates the Szekeres metric is written as

$$\mathrm{d}s^2 = c^2\mathrm{d}t^2 - \mathrm{e}^{2\alpha}\mathrm{d}r^2 - \mathrm{e}^{2\beta}(\mathrm{d}x^2 + \mathrm{d}y^2), \qquad (2.1)$$

where $\alpha \equiv \alpha(t, r, x, y)$ and $\beta \equiv \beta(t, r, x, y)$ are two functions which will be determined by the field equations.

Szekeres solutions are divided into two categories depending upon the value of β' where the prime denotes derivative with respect to r. The class II family, where $\beta' = 0$, is a simultaneous generalization of the Friedmann and Kantowski-Sachs models [26]. Its spherically symmetric limit is the Datt-Ruban solution [27,28]. The class I family where β' is nonzero contains the LTB solution as a spherically symmetric limit.

Therefore, we choose this class of solutions to study Szekeres models. After a change of parameters more convenient for our purpose [29] and after solving Einstein's equations, the class I Szekeres metric can be written as

$$\mathrm{d}s^2 = c^2\mathrm{d}t^2 - \frac{(\Phi' - \Phi E'/E)^2}{\epsilon - k}\mathrm{d}r^2 - \frac{\Phi^2}{E^2}(\mathrm{d}x^2 + \mathrm{d}y^2), \qquad (2.2)$$

where $\epsilon = 0, \pm 1$, Φ is a function of t and r, k is a function of r, and

$$E = \frac{S}{2}\left[\left(\frac{x - P}{S}\right)^2 + \left(\frac{y - Q}{S}\right)^2 + \epsilon\right], \qquad (2.3)$$

with $S(r)$, $P(r)$, $Q(r)$, functions of r.

From (2.2) it can be seen that all three Friedmann limits (hyperbolic, flat, and spherical) can be achieved only in the case where $\epsilon = +1$. This is induced by the requirement of a Lorentzian signature for the metric. Since we are interested in studying such an inhomogeneous model which becomes homogeneous at large scales, i.e., before the last scattering, we consider only the $\epsilon = +1$ case. It is called the quasispherical Szekeres solution. This QSS solution can be imagined as a LTB model generalization in which the constant mass spheres are nonconcentric. For the QSS

metric with $\epsilon = +1$ (2.2) the Einstein equations reduce to the following two:

$$\frac{1}{c^2}\dot{\Phi}^2 = \frac{2M}{\Phi} - k + \frac{1}{3}\Lambda\Phi^2, \tag{2.4}$$

where the dot denotes derivation with respect to t, Λ is the cosmological constant, and $M(r)$ is an arbitrary function of r related to the density ρ via

$$\kappa\rho c^2 = \frac{2M' - 6ME'/E}{\Phi^2(\Phi' - \Phi E'/E)}, \tag{2.5}$$

where $\kappa = 8\pi G/c^4$.

The integration of (2.4) yields

$$\pm\int_0^{\Phi} \frac{\mathrm{d}\tilde{\Phi}}{\sqrt{-k + 2M/\tilde{\Phi} + \frac{1}{3}\Lambda\tilde{\Phi}^2}} = c[t - t_B(r)], \tag{2.6}$$

where $t_B(r)$ is an arbitrary function which is called bang time function and it defines the initial moment of evolution. When $t_B' \neq 0$, i.e., in general, this singularity instant is position dependent, as in the LTB model. The plus sign applies for expanding regions. The minus sign applies for collapsing regions. Here, we study the QSS model with $\Lambda = 0$.

All the equations written so far are covariant under coordinate transformations of the form $\tilde{r} = g(r)$. It means that one of the six functions $k(r)$, $S(r)$, $P(r)$, $Q(r)$, $M(r)$, or $t_B(r)$ can be fixed at our convenience by the choice of g. Hence, each Szekeres solution is fully determined by only five functions of r and a coordinate choice. In the BSQSS model, these functions are S, P, Q, M, and t_B, and the coordinate choice is $\Phi(t_{ls}, r) = r$, where the radial coordinate is the areal radius at the last scattering instant, t_{ls}.

III. REDSHIFT AND REDSHIFT DRIFT IN QSS MODELS

As stressed in the Introduction, our first aim was to compute the redshift drift for the BSQSS model and to compare it to that in the A09 model. However, while calculating this drift, we first computed the redshift and found that it was negative, i.e., a blueshift. Since a cosmological blueshift is not observed in the universe, this is enough to rule out the BSQSS model as a physical cosmological model. Hence, the redshift drift, which, in this model, would be a blueshift drift, should also be unphysical. However, we do not claim that such a blueshift is a QSS model general feature. Hence, since, to our knowledge, the equations and method to calculate the redshift drift for the most general QSS models have never been displayed in the literature, we present them in this section, so that they might be used in future works to discriminate between physical QSS models and other models.

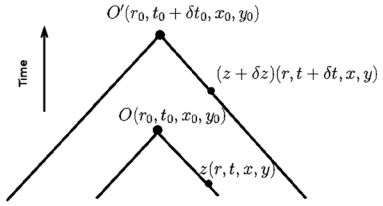

FIG. 1. The redshift drift δz of a source, initially at a redshift z on the past light cone of an observer at O, as measured by the same observer at O' after an elapsed time δt_0 of the observer's proper time.

A. Definition of the redshift drift

The redshift drift is the temporal change in the redshift measured by an observer looking at the same comoving source on her past light cone at different proper time. Its mathematical definition is $\delta z/\delta t_0$ which is explained schematically in Fig. 1.

The redshift drift has first been calculated by Sandage [22] and McVittie [23] in 1962 for FLRW models. Its expression in these models is given by

$$\frac{\delta z}{1+z} = H_0\delta t_0\left(1 - \frac{H(z)}{(1+z)H_0}\right), \tag{3.1}$$

where H_0 and $H(z)$ are Hubble expansion rates at redshifts 0 or scale factor $(a_0 = 1)$ and z, respectively. Since it is a quantity evolving off the observer's past light cone, it can be used to suppress the degeneracy between models reproducing the same cosmological data on this light cone. It has been calculated for some LTB models [30,31], an axially symmetric QSS model [24], Stephani models [32], as well as in varying speed of light (VSL) theory [33] with no dark energy and many other cosmological models [34–44]. Since axially symmetric QSS models [25] are not realistic universe models, we give two new recipes for calculating the redshift drift for QSS models which do not exhibit any symmetry.

B. The equations for the redshift and the redshift drift

The geodesic equations for the QSS model in (t, r, x, y) coordinates are [45]

$$c^2\frac{\mathrm{d}^2t}{\mathrm{d}s^2} + \frac{\Phi_{,tr} - \Phi_{,t}E_{,r}/E}{1-k}(\Phi_{,r} - \Phi E_{,r}/E)\left(\frac{\mathrm{d}r}{\mathrm{d}s}\right)^2 + \frac{\Phi\Phi_{,t}}{E^2}\left[\left(\frac{\mathrm{d}x}{\mathrm{d}s}\right)^2 + \left(\frac{\mathrm{d}y}{\mathrm{d}s}\right)^2\right] = 0, \tag{3.2}$$

$$\frac{d^2r}{ds^2}+2c\frac{\Phi_{,tr}-\Phi_{,t}E_{,r}/E}{\Phi_{,r}-\Phi E_{,r}/E}\frac{dt}{ds}\frac{dr}{ds}+\left(\frac{\Phi_{,rr}-\Phi E_{,rr}/E}{\Phi_{,r}-\Phi E_{,r}/E}-\frac{E_{,r}}{E}+\frac{1}{2}\frac{k_{,r}}{1-k}\right)\left(\frac{dr}{ds}\right)^2+2\frac{\Phi}{E^2}\frac{E_{,r}E_{,x}-EE_{,xr}}{\Phi_{,r}-\Phi E_{,r}/E}\frac{dr}{ds}\frac{dx}{ds}+2\frac{\Phi}{E^2}\frac{(E_{,r}E_{,y}-EE_{,yr})}{\Phi_{,r}-\Phi E_{,r}/E}\frac{dr}{ds}\frac{dy}{ds}-\frac{\Phi}{E^2}\frac{1-k}{\Phi_{,r}-\Phi E_{,r}/E}\left[\left(\frac{dx}{ds}\right)^2+\left(\frac{dy}{ds}\right)^2\right]=0, \tag{3.3}$$

$$\frac{d^2x}{ds^2}+2c\frac{\Phi_{,t}}{\Phi}\frac{dt}{ds}\frac{dx}{ds}-\frac{1}{\Phi}\frac{\Phi_{,r}-\Phi E_{,r}/E}{1-k}(E_{,r}E_{,x}-EE_{,xr})\left(\frac{dr}{ds}\right)^2+\frac{2}{\Phi}\left(\Phi_{,r}-\Phi\frac{E_{,r}}{E}\right)\frac{dr}{ds}\frac{dx}{ds}-\frac{E_{,x}}{E}\left(\frac{dx}{ds}\right)^2-2\frac{E_{,y}}{E}\frac{dx}{ds}\frac{dy}{ds}+\frac{E_{,x}}{E}\left(\frac{dy}{ds}\right)^2=0, \tag{3.4}$$

$$\frac{d^2y}{ds^2}+2c\frac{\Phi_{,t}}{\Phi}\frac{dt}{ds}\frac{dy}{ds}-\frac{1}{\Phi}\frac{\Phi_{,r}-\Phi E_{,r}/E}{1-k}(E_{,r}E_{,y}-EE_{,yr})\left(\frac{dr}{ds}\right)^2+\frac{2}{\Phi}\left(\Phi_{,r}-\Phi\frac{E_{,r}}{E}\right)\frac{dr}{ds}\frac{dy}{ds}+\frac{E_{,y}}{E}\left(\frac{dx}{ds}\right)^2-2\frac{E_{,x}}{E}\frac{dx}{ds}\frac{dy}{ds}-\frac{E_{,y}}{E}\left(\frac{dy}{ds}\right)^2=0. \tag{3.5}$$

And the null condition is

$$c^2\left(\frac{dt}{ds}\right)^2-\frac{(\Phi_{,r}-\Phi E_{,r}/E)^2}{1-k}\left(\frac{dr}{ds}\right)^2-\frac{\Phi^2}{E^2}\left(\left(\frac{dx}{ds}\right)^2+\left(\frac{dy}{ds}\right)^2\right)=0. \tag{3.6}$$

Now, we choose the r coordinate as the affine parameter, using the following transformation relation:

$$\frac{d^2x^\mu}{ds^2}=\left(\frac{dr}{ds}\right)^2\frac{d^2x^\mu}{dr^2}+\frac{d^2r}{ds^2}\frac{dx^\mu}{dr}. \tag{3.7}$$

Then, from (3.3) we have

$$\frac{d^2r}{ds^2}=\left(\frac{dr}{ds}\right)^2\left\{-2c\frac{\Phi_{01}}{\Phi_1}\frac{dt}{dr}-\left(\frac{\Phi_{11}}{\Phi_1}-\frac{E_{,r}}{E}+\frac{1}{2}\frac{k_{,r}}{1-k}\right)-2\frac{\Phi}{E^2}\frac{E_{12}}{\Phi_1}\frac{dx}{dr}-2\frac{\Phi}{E^2}\frac{E_{13}}{\Phi_1}\frac{dy}{dr}+\frac{\Phi}{E^2}\frac{1-k}{\Phi_1}\Sigma\right\}=U(t,r,x,y)\left(\frac{dr}{ds}\right)^2, \tag{3.8}$$

where

$$\Phi_1=\Phi_{,r}-\Phi E_{,r}/E, \tag{3.9}$$

$$\Phi_{01}=\Phi_{,tr}-\Phi_{,t}E_{,r}/E, \tag{3.10}$$

$$\Phi_{11}=\Phi_{,rr}-\Phi E_{,rr}/E, \tag{3.11}$$

$$E_{12}=E_{,r}E_{,x}-EE_{,xr}, \tag{3.12}$$

$$E_{13}=E_{,r}E_{,y}-EE_{,yr}, \tag{3.13}$$

$$\Sigma=\left(\frac{dx}{dr}\right)^2+\left(\frac{dy}{dr}\right)^2, \tag{3.14}$$

and

$$U=-2c\frac{\Phi_{01}}{\Phi_1}\frac{dt}{dr}-\frac{\Phi_{11}}{\Phi_1}+\frac{E_{,r}}{E}-\frac{1}{2}\frac{k_{,r}}{1-k}-2\frac{\Phi}{E^2}\frac{E_{12}}{\Phi_1}\frac{dx}{dr}-2\frac{\Phi}{E^2}\frac{E_{13}}{\Phi_1}\frac{dy}{dr}+\frac{\Phi}{E^2}\frac{1-k}{\Phi_1}\Sigma. \tag{3.15}$$

The above transformation will bring the geodesic equations and the null condition equation in the following form:

$$c^2\frac{d^2t}{dr^2}+\frac{\Phi_1\Phi_{01}}{1-k}+\frac{\Phi\Phi_{,t}}{E^2}\Sigma+cU\frac{dt}{dr}=0, \tag{3.16}$$

$$\frac{d^2x}{dr^2}+2c\frac{\Phi_{,t}}{\Phi}\frac{dt}{dr}\frac{dx}{dr}-\frac{1}{\Phi}\frac{\Phi_1}{1-k}E_{12}+\frac{2\Phi_1}{\Phi}\frac{dx}{dr}-\frac{E_{,x}}{E}\left(\frac{dx}{dr}\right)^2-2\frac{E_{,y}}{E}\frac{dx}{dr}\frac{dy}{dr}+\frac{E_{,x}}{E}\left(\frac{dy}{dr}\right)^2+U\frac{dx}{dr}=0, \tag{3.17}$$

$$\frac{d^2y}{dr^2}+2c\frac{\Phi_{,t}}{\Phi}\frac{dt}{dr}\frac{dy}{dr}-\frac{1}{\Phi}\frac{\Phi_1}{1-k}E_{13}+\frac{2\Phi_1}{\Phi}\frac{dy}{dr}+\frac{E_{,y}}{E}\left(\frac{dx}{dr}\right)^2-2\frac{E_{,x}}{E}\frac{dx}{dr}\frac{dy}{dr}-\frac{E_{,y}}{E}\left(\frac{dy}{dr}\right)^2+U\frac{dy}{dr}=0, \tag{3.18}$$

$$c^2\left(\frac{dt}{dr}\right)^2-\frac{\Phi_1^2}{1-k}-\frac{\Phi^2}{E^2}\Sigma=0. \tag{3.19}$$

The equation for the redshift in QSS models is [26,45]

$$\frac{\mathrm{d}z}{\mathrm{d}r} = \frac{1+z}{c}\frac{\dot{\Phi}' - \dot{\Phi}E'/E}{\sqrt{1-k}}. \tag{3.20}$$

Initially the observer's coordinates are $(t(s_o), r(s_o), x(s_o), y(s_o))$, which we write (t_0, r_0, x_0, y_0), and the source coordinates are $(t(s_e), r(s_e), x(s_e), y(s_e))$, which we write (t_e, r_e, x_e, y_e).

Substituting $t = t + \delta t$ in (3.19), and keeping terms only up to first order in δt, we get

$$c^2\left(\frac{\mathrm{d}(t+\delta t)}{\mathrm{d}r}\right)^2 - \frac{(\Phi_1 + \dot{\Phi}_1\delta t)^2}{1-k} - \frac{(\Phi + \dot{\Phi}\delta t)^2}{E^2}\Sigma = 0. \tag{3.21}$$

Now subtracting (3.19) from (3.21), and still keeping terms only up to first order in δt, we get

$$c^2\frac{\mathrm{d}t}{\mathrm{d}r}\frac{\mathrm{d}\delta t}{\mathrm{d}r} - \frac{\Phi_1\dot{\Phi}_1}{1-k}\delta t - \frac{\Phi\dot{\Phi}}{E^2}\delta t\Sigma = 0. \tag{3.22}$$

Substituting $z = z + \delta z$ and $t = t + \delta t$ in (3.20) we obtain

$$\frac{\mathrm{d}(z+\delta z)}{\mathrm{d}r} = \frac{1+z+\delta z}{c}\frac{\dot{\Phi}'(t+\delta t) - \dot{\Phi}(t+\delta t)E'/E}{\sqrt{1-k}}. \tag{3.23}$$

Subtracting (3.20) from (3.23), and keeping terms only up to first order in δt and δz, we get

$$\frac{\mathrm{d}(\delta z)}{\mathrm{d}r} = \frac{1+z}{c\sqrt{1-k}}\dot{\Phi}_{01}\delta t + \frac{\delta z}{c\sqrt{1-k}}\Phi_{01}. \tag{3.24}$$

We will solve (3.24) together with (3.16)–(3.18) and (3.22) to get the redshift drift in QSS models.

The redshift drift can also be calculated by the following method.

Initially the observer's coordinates are $(t(s_o), r(s_o), x(s_o), y(s_o))$, which we write (t_0, r_0, x_0, y_0), and the source coordinates are $(t(s_e), r(s_e), x(s_e), y(s_e))$, which we write (t_e, r_e, x_e, y_e). The redshift of this source is z given by

$$1 + z = \frac{k_t^e}{k_t^o}, \tag{3.25}$$

$$= \frac{\mathrm{d}t/\mathrm{d}s|_{s=s_e}}{\mathrm{d}t/\mathrm{d}s|_{s=s_o}}. \tag{3.26}$$

After some proper time elapse δt_0 at the observer's location, the observer's coordinates become $(t_0 + \delta t_0, r_0, x_0, y_0)$, and the source coordinates become $(t_e + \delta t(s_e), r_e, x_e, y_e)$. Since we are working with comoving coordinates, r, x, and y do not change.

Substituting $t = t + \delta t$ in (3.2)–(3.5), we get

$$c^2\frac{\mathrm{d}^2(t+\delta t)}{\mathrm{d}s^2} + \left(\frac{\Phi_{,tr} - \Phi_{,t}E_{,r}/E}{1-k}(\Phi_{,r} - \Phi E_{,r}/E)\right) \times (t+\delta t, r, x, y)\left(\frac{\mathrm{d}r}{\mathrm{d}s}\right)^2 + \left(\frac{\Phi\Phi_{,t}}{E^2}\right)(t+\delta t, r, x, y) \times \left[\left(\frac{\mathrm{d}x}{\mathrm{d}s}\right)^2 + \left(\frac{\mathrm{d}y}{\mathrm{d}s}\right)^2\right] = 0, \tag{3.27}$$

$$\frac{\mathrm{d}^2r}{\mathrm{d}s^2} + 2c\left(\frac{\Phi_{,tr} - \Phi_{,t}E_{,r}/E}{\Phi_{,r} - \Phi E_{,r}/E}\right)(t+\delta t, r, x, y)\frac{\mathrm{d}(t+\delta t)}{\mathrm{d}s}\frac{\mathrm{d}r}{\mathrm{d}s} + \left(\left(\frac{\Phi_{,rr} - \Phi_{,r}E_{,r}/E - \Phi E_{,rr}/E + \Phi(E_{,r}/E)^2}{\Phi_{,r} - \Phi E_{,r}/E}\right) \times (t+\delta t, r, x, y) + \frac{1}{2}\frac{k_{,r}}{1-k}\right)\left(\frac{\mathrm{d}r}{\mathrm{d}s}\right)^2 + 2\left(\frac{\Phi}{E^2}\frac{E_{,r}E_{,x} - EE_{,xr}}{\Phi_{,r} - \Phi E_{,r}/E}\right)(t+\delta t, r, x, y)\frac{\mathrm{d}r}{\mathrm{d}s}\frac{\mathrm{d}x}{\mathrm{d}s} + 2\left(\frac{\Phi}{E^2}\frac{(E_{,r}E_{,y} - EE_{,yr})}{\Phi_{,r} - \Phi E_{,r}/E}\right) \times (t+\delta t, r, x, y)\frac{\mathrm{d}r}{\mathrm{d}s}\frac{\mathrm{d}y}{\mathrm{d}s} - \left(\frac{\Phi}{E^2}\frac{1-k}{\Phi_{,r} - \Phi E_{,r}/E}\right)(t+\delta t, r, x, y)\left[\left(\frac{\mathrm{d}x}{\mathrm{d}s}\right)^2 + \left(\frac{\mathrm{d}y}{\mathrm{d}s}\right)^2\right] = 0, \tag{3.28}$$

$$\frac{\mathrm{d}^2x}{\mathrm{d}s^2} + 2c\frac{\Phi_{,t}}{\Phi}(t+\delta t, r)\frac{\mathrm{d}(t+\delta t)}{\mathrm{d}s}\frac{\mathrm{d}x}{\mathrm{d}s} - \left(\frac{1}{\Phi}\frac{\Phi_{,r} - \Phi E_{,r}/E}{1-k} \times (E_{,r}E_{,x} - EE_{,xr})\right)(t+\delta t, r, x, y)\left(\frac{\mathrm{d}r}{\mathrm{d}s}\right)^2 + 2\left(\frac{\Phi_{,r}}{\Phi}(t+\delta t, r) - \frac{E_{,r}}{E}\right)\frac{\mathrm{d}r}{\mathrm{d}s}\frac{\mathrm{d}x}{\mathrm{d}s} - \frac{E_{,x}}{E}\left(\frac{\mathrm{d}x}{\mathrm{d}s}\right)^2 - 2\frac{E_{,y}}{E}\frac{\mathrm{d}x}{\mathrm{d}s}\frac{\mathrm{d}y}{\mathrm{d}s} + \frac{E_{,x}}{E}\left(\frac{\mathrm{d}y}{\mathrm{d}s}\right)^2 = 0, \tag{3.29}$$

$$\frac{\mathrm{d}^2y}{\mathrm{d}s^2} + 2c\frac{\Phi_{,t}}{\Phi}(t+\delta t, r)\frac{\mathrm{d}(t+\delta t)}{\mathrm{d}s}\frac{\mathrm{d}y}{\mathrm{d}s} - \left(\frac{1}{\Phi}\frac{\Phi_{,r} - \Phi E_{,r}/E}{1-k} \times (E_{,r}E_{,y} - EE_{,yr})\right)(t+\delta t, r, x, y)\left(\frac{\mathrm{d}r}{\mathrm{d}s}\right)^2 + 2\left(\frac{\Phi_{,r}}{\Phi}(t+\delta t, r) - \frac{E_{,r}}{E}\right)\frac{\mathrm{d}r}{\mathrm{d}s}\frac{\mathrm{d}y}{\mathrm{d}s} + \frac{E_{,y}}{E}\left(\frac{\mathrm{d}x}{\mathrm{d}s}\right)^2 - 2\frac{E_{,x}}{E}\frac{\mathrm{d}x}{\mathrm{d}s}\frac{\mathrm{d}y}{\mathrm{d}s} - \frac{E_{,y}}{E}\left(\frac{\mathrm{d}y}{\mathrm{d}s}\right)^2 = 0. \tag{3.30}$$

Subtracting (3.2) from (3.27), and keeping only the first order terms in δt, we obtain

$$c^2\frac{\mathrm{d}^2\delta t}{\mathrm{d}s^2}+\frac{\partial}{\partial t}\left(\frac{\Phi_{,tr}-\Phi_{,t}E_{,r}/E}{1-k}\left(\Phi_{,r}-\Phi\frac{E_{,r}}{E}\right)\right)\delta t\left(\frac{\mathrm{d}r}{\mathrm{d}s}\right)^2+\frac{\partial}{\partial t}\left(\frac{\Phi\Phi_{,t}}{E^2}\right)\delta t\left[\left(\frac{\mathrm{d}x}{\mathrm{d}s}\right)^2+\left(\frac{\mathrm{d}y}{\mathrm{d}s}\right)^2\right]=0. \tag{3.31}$$

Now we want to calculate the change in redshift δz which would be observed after a proper time elapse δt_0 at the observer's location. We proceed as follows.

The new redshift $(z+\delta z)$ is given by

$$1+z+\delta z=\frac{\mathrm{d}(t+\delta t)/\mathrm{d}s|_{s=s_e}}{\mathrm{d}(t+\delta t)/\mathrm{d}s|_{s=s_o}}. \tag{3.32}$$

Subtracting (3.26) from (3.32), we obtain

$$\delta z=\frac{\mathrm{d}(t+\delta t)/\mathrm{d}s|_{s=s_e}}{\mathrm{d}(t+\delta t)/\mathrm{d}s|_{s=s_o}}-\frac{\mathrm{d}t/\mathrm{d}s|_{s=s_e}}{\mathrm{d}t/\mathrm{d}s|_{s=s_o}}, \tag{3.33}$$

$$\delta z=\frac{(\mathrm{d}t/\mathrm{d}s+\mathrm{d}\delta t/\mathrm{d}s)|_{s=s_e}}{(\mathrm{d}t/\mathrm{d}s+\mathrm{d}\delta t/\mathrm{d}s)|_{s=s_o}}-\frac{\mathrm{d}t/\mathrm{d}s|_{s=s_e}}{\mathrm{d}t/\mathrm{d}s|_{s=s_o}}, \tag{3.34}$$

$$\delta z=\frac{\mathrm{d}t/\mathrm{d}s|_{s=s_e}}{\mathrm{d}t/\mathrm{d}s|_{s=s_o}}\left(\frac{1+\frac{\mathrm{d}\delta t/\mathrm{d}s}{\mathrm{d}t/\mathrm{d}s}|_{s=s_e}}{1+\frac{\mathrm{d}\delta t/\mathrm{d}s}{\mathrm{d}t/\mathrm{d}s}|_{s=s_o}}\right)-\frac{\mathrm{d}t/\mathrm{d}s|_{s=s_e}}{\mathrm{d}t/\mathrm{d}s|_{s=s_o}}, \tag{3.35}$$

$$\delta z=(1+z)\left(\frac{\frac{\mathrm{d}\delta t/\mathrm{d}s}{\mathrm{d}t/\mathrm{d}s}|_{s=s_e}-\frac{\mathrm{d}\delta t/\mathrm{d}s}{\mathrm{d}t/\mathrm{d}s}|_{s=s_o}}{1+\frac{\mathrm{d}\delta t/\mathrm{d}s}{\mathrm{d}t/\mathrm{d}s}|_{s=s_o}}\right). \tag{3.36}$$

We also write Eq. (3.36) for the redshift drift as

$$\delta z=(1+z)\left(\frac{\frac{\mathrm{d}\delta t/\mathrm{d}r}{\mathrm{d}t/\mathrm{d}r}|_{r=r_e}-\frac{\mathrm{d}\delta t/\mathrm{d}r}{\mathrm{d}t/\mathrm{d}r}|_{r=r_o}}{1+\frac{\mathrm{d}\delta t/\mathrm{d}r}{\mathrm{d}t/\mathrm{d}r}|_{r=r_o}}\right). \tag{3.37}$$

This is another equation to calculate the redshift drift in any QSS model. By solving (3.37) one can compute the change in redshift of a source at (t_e, r_e, x_e, y_e) after a δt_0 proper time has elapsed at the observer's initial location in spacetime, (t_o, r_o, x_o, y_o). The quantities $\mathrm{d}\delta t/\mathrm{d}r$ and $\mathrm{d}t/\mathrm{d}r$ appearing in (3.37) are obtained by solving (3.16)–(3.19) simultaneously.

In the first method we have to solve five first order with degree two equations simultaneously to obtain the redshift drift, whereas in the second method we have to solve only three equations simultaneously to get the redshift drift. Therefore, the second method is better in any case.

C. Calculation of the function $k(r)$

Since we know $M(r)$, the function $k(r)$ is needed to compute Φ from the parametric solution of (2.4) we can obtain when $\Lambda=0$, once we have determined the sign of $k(r)$. There are two different methods for calculating $k(r)$ depending on the value of the $t_B(r)$ function.

1. $t_B(r)\neq 0$

In this case, we use the parametric method. However, there are three different parametric solutions depending on the sign of $k(r)$:

(i) $k>0$

$$\Phi(t,r)=\frac{M}{k}(1-\cos\eta) \tag{3.38}$$

and

$$t-t_B(r)=\frac{M}{k^{3/2}}(\eta-\sin\eta). \tag{3.39}$$

(ii) $k=0$

$$\Phi(t,r)=\left[\frac{9}{2}M(t-t_B(r))^2\right]^{1/3}. \tag{3.40}$$

(iii) $k<0$

$$\Phi(r,t)=\frac{M}{(-k)}(\cosh\eta-1) \tag{3.41}$$

and

$$t-t_B(r)=\frac{M}{(-k)^{3/2}}(\sinh\eta-\eta), \tag{3.42}$$

where $\eta(t,r)$ is the parameter.

We do not know *a priori* what is the $k(r)$ sign. Therefore, we have to try the above three solutions at random. Our coordinate choice is $\Phi(t_0,r)=r$. This choice helps us to determine the function $k(r)$ as following.

The case $k=0$ is the easiest to deal with. Setting $t=t_0$ in (3.40) and replacing $M(r)$ and $t_B(r)$ by their expressions, and $\Phi(t_0,r)$ by r, we see at once whether (3.40) is fulfilled for some given r values. There might indeed be cases when k vanishes for some r value(s) and k changes sign (or not) at this (these) value(s). In these cases, we have to test $k<0$ and $k>0$ for the different r ranges, between the values where k is null. If k vanishes nowhere, we just guess the sign of k for all the r values and proceed as follows.

We give here the reasoning for $k<0$. Since at $t=t_0$, $\Phi(t_0,r)=r$, and $\eta(t_0,r)=\eta_0(r)$, we set $t=t_0$ in (3.41) and (3.42) and eliminate $k(r)$ between both. We obtain

$$-k=\frac{M}{r}(\cosh\eta_0-1), \tag{3.43}$$

$$t_0-t_B(r)=\frac{r^{3/2}}{M^{1/2}}\frac{(\sinh\eta_0-\eta_0)}{(\cosh\eta_0-1)^{3/2}}. \tag{3.44}$$

We keep the nonvanishing root of (3.44) for $\eta_0(r)$, and we substitute it in (3.41) where we have set $t = t_0$ to get $k(r)$.

An analogous method applies for the case $k > 0$.

2. $t_B(r) = 0$

In this case, we do not need to guess *a priori* the sign of $k(r)$. It proceeds directly from the calculations. However, we must guess the sign in front of the integral in (2.6), since we do not know whether the region of the model we are considering is expanding or collapsing. Since we are supposed to study a cosmological model, we could guess that the plus sign applies, but we will see in the following that the BSQSS model region of interest is blueshifted and therefore collapsing.

As an example, we describe this method with the plus sign. The method with the minus sign follows easily. We set $t = t_0$ and $\Lambda = t_B(r) = 0$ in (2.6) with the plus sign and obtain

$$\int_0^r \frac{\mathrm{d}\tilde{\Phi}}{\sqrt{-k(r) + 2M(r)/\tilde{\Phi}}} = ct_0. \tag{3.45}$$

To avoid divergences due to the $1/\tilde{\Phi}$ term, we multiply the integrand by $\sqrt{\tilde{\Phi}/\tilde{\Phi}}$. Equation (3.45) becomes

$$\int_0^r \sqrt{\frac{\tilde{\Phi}}{-k(r)\tilde{\Phi} + 2M(r)}}\mathrm{d}\tilde{\Phi} = ct_0. \tag{3.46}$$

Now, for a given r value,

(i) We choose a $k(r)$ value in this function definition interval, i.e., $-\infty < k < 1$. We span this interval with k values separated by some given step. Since we cannot span all this interval toward negative values, we begin with taking as limits $-1 < k < 1$ (if necessary, we try an extended interval afterwards). We try first $k = -1$, and then $k = 1$, since we will use an interpolation method to find k.

(ii) We insert each k value, and that of M for the given r value, in the integral of (3.46) which we integrate with, e.g., the trapezium method, with a r/n integration step. We write $\int_0^r \sqrt{\frac{\tilde{\Phi}}{-k\tilde{\Phi}+2M}}\mathrm{d}\tilde{\Phi} = \sum_{i=1}^n \sqrt{\frac{\tilde{\Phi}_i}{-k\tilde{\Phi}_i+2M}}\delta\tilde{\Phi} = I(r)$, with $\delta\tilde{\Phi} = r/n$ and $\tilde{\Phi}_i = ir/n$.

(iii) Then, we check whether $I(r) = ct_0$. If this is the case, that means that the k value chosen corresponds actually to the given r value. If not, we try another value for k using an interpolation method and so on. By this method, we are able to check whether the interval $-1 < k < 1$ is satisfactory or whether we need to extend it toward more negative values.

We reiterate the above calculation for a number of r values spanning the light cone section of interest.

D. The algorithm

In order to calculate the redshift and the redshift drift, we proceed in the following manner:

(1) Once $k(r)$ is determined by one of the above methods, we use the corresponding parametric solution for Φ to find $\Phi(t, r)$ and its derivatives on the past light cone.

(2) We substitute the Σ value from (3.19) into the geodesic equations (3.16)–(3.18) to transform them into null geodesic equations.

(3) Then we split the three second order null geodesic equations thus obtained into six first order ordinary equations.

(4) We find $t(r)$, $x(r)$, $y(r)$, and their first order derivatives on the past light cone by numerically solving these null geodesic equations. The initial conditions at the current observer where $r = r_o$ are chosen as $t = t_0$, $x = x_0$, $y = y_0$, $\mathrm{d}x/\mathrm{d}r = \mathrm{d}x/\mathrm{d}r|_0$, and $\mathrm{d}y/\mathrm{d}r = \mathrm{d}y/\mathrm{d}r|_0$, and the initial condition for $\mathrm{d}t/\mathrm{d}r$ is determined from the null condition.

(5) Then we find the redshift z by numerically integrating (3.26).

(6) After having found z, we find δt and δz by numerically solving (3.22) and (3.24) together.

(7) Then we find the redshift drift $\delta z/\delta t_0$ with $\delta t_0 = 10$ years. δt_0 has been chosen as 10 years to observe the change in redshift drift in 10 years. For δt_0 less than this, the change would be too small to observe and for δt_0 much larger than this, it would not be possible to measure the redshift drift with the upcoming satellites which are planned for years of the order of 10 only.

IV. COMPUTATION OF THE REDSHIFT AND THE REDSHIFT DRIFT IN THE BSQSS MODEL

A. The BSQSS model

The BSQSS model is defined at the last scattering surface by specifying five among its six arbitrary functions of r and one coordinate choice. The five functions are $t_B(r), M(r), S(r), P(r), Q(r)$.

We have chosen this model because on spatial averaging, it has been shown in Ref. [20] that the averaged model reproduces qualitatively the minimum void (MV) model of Ref. [21] which fits SN Ia and WMAP data and is consistent with the local H_0 value.

In the BSQSS model, the bang time function, $t_B(r)$, is null and the $M(r)$ function is given by

$$M(r) = 4\pi\frac{G}{c^2}\int_0^r \rho_b(1 + \delta\bar{\rho})\bar{r}^2\mathrm{d}\bar{r},$$

where $\delta\bar{\rho} = -0.005\mathrm{e}^{-(\ell/100)^2} + 0.0008\mathrm{e}^{-[(\ell-50)/35]^2} + 0.0005\mathrm{e}^{-[(\ell-115)/60]^2} + 0.0002\mathrm{e}^{-[(\ell-140)/55]^2}$, and $\ell \equiv r/1\,\mathrm{kpc}$.

The functions Q, P, and S are defined as follows:
$S = 1 \Rightarrow S' = 0$,
$\mathcal{D} = 1.05(1+r)^{-0.99}\mathrm{e}^{-0.004r}$,
$Q' = \mathcal{D}$, $P' = 0$ for $\ell \leq 27$,
$Q' = -\mathcal{D}$, $P' = 0$ for $27 < \ell \leq 35$,
$Q' = 0$, $P' = -\mathcal{D}$ for $35 < \ell \leq 41$,
$Q' = 0$, $P' = \mathcal{D}$ for $41 < \ell \leq 51.5$,
$Q' = 0.88\mathcal{D}$, $P' = -0.5\mathcal{D}$ for $51.5 < \ell \leq 61$,
$Q' = 0.71\mathcal{D}$, $P' = 0.71\mathcal{D}$ for $61 < \ell \leq 69$,
$Q' = 0$, $P' = -\mathcal{D}$ for $69 < \ell \leq 77$,
$Q' = -\mathcal{D}$, $P' = 0$ for $77 < \ell \leq 86.5$,
$Q' = 0.74\mathcal{D}$, $P' = -0.74\mathcal{D}$ for $86.5 < \ell \leq 96$,
$Q' = \mathcal{D}$, $P' = \mathcal{D}$ for $96 < \ell \leq 102$,
$Q' = -\mathcal{D}$, $P' = 0$ for $102 < \ell \leq 115$,
$Q' = \mathcal{D}$, $P' = 0$ for $115 < \ell \leq 129$,
$Q' = 0$, $P' = -\mathcal{D}$ for $\ell > 129$.

B. Calculation of the function $k(r)$

Since $t_B(r) = 0$, we could have used the second method described in Sec. III C to compute $k(r)$. However, we faced a problem in our numerical calculations since an *a priori* expanding cosmological model was not compatible with the BSQSS model. Of course, we could have changed the sign in (3.45), but we found that the first method used less CPU time, since the same equations give $k(r)$ and $\Phi(t, r)$.

Therefore, we switched to the first method and found that the equations with $k < 0$ for all r gave us a proper solution to our problem. The $k(r)$ function is displayed in Fig. 2.

C. The redshift

We have run our code over a huge number of initial conditions, and we have always found the same qualitative results for the redshift, in particular its sign.

For Fig. 3 displayed here, the initial conditions at the current observer where $r = r_o = 100$ Mpc are

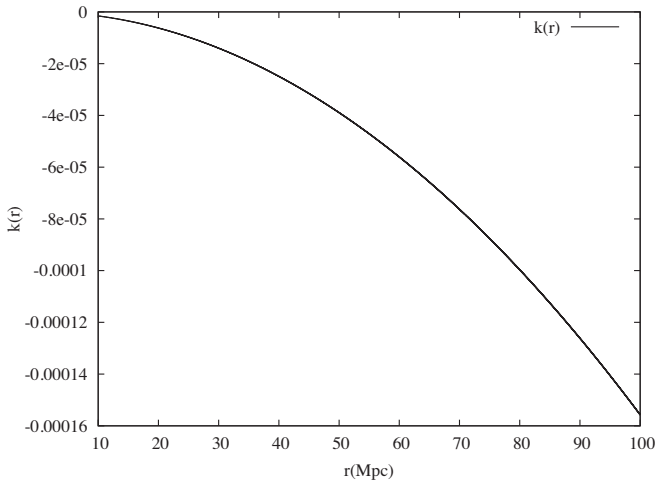

FIG. 2. The $k(r)$ function in the BSQSS model.

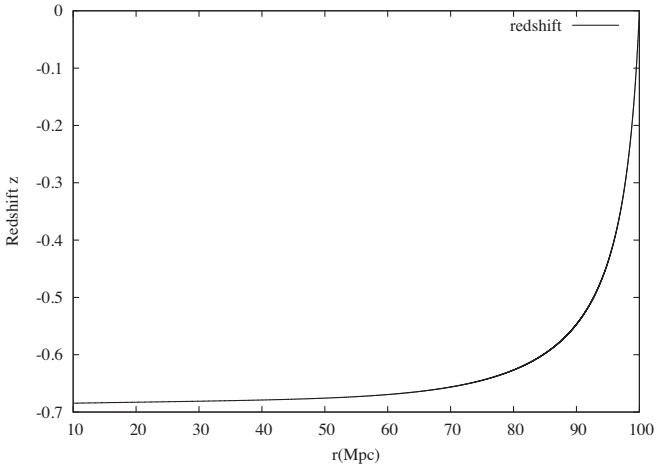

FIG. 3. The negative redshift (blueshift) as a function of the comoving distance r for the BSQSS model.

$$t = t_o = 13.7 \text{ Gyr}, \tag{4.1}$$

$$x = 0.00001, \tag{4.2}$$

$$y = 0.00001, \tag{4.3}$$

$$\mathrm{d}x/\mathrm{d}r = 0.0001, \tag{4.4}$$

$$\mathrm{d}y/\mathrm{d}r = 0.0001, \tag{4.5}$$

and the initial condition for $\mathrm{d}t/\mathrm{d}r$ is determined from the null condition.

Figure 3 shows the redshift as a function of the comoving distance r in the BSQSS model. This redshift is found to be negative which means that the light rays reaching the observer in a BSQSS universe are blueshifted. We observe this blueshift because the observer's location is not at this model origin which is at the last scattering surface. Since in this model the universe is expanding away from this origin, the sources are coming toward the observer which is at $t = t_0$ and $r_0 = 100$ Mpc. Hence, the light rays are blueshifted. Since such a cosmological blueshift is not observed in the universe, this means that the nonaveraged BSQSS model is ruled out as a cosmological model.

D. The redshift drift (blueshift drift)

For completeness, we have used the above described recipe to compute the redshift drift (which is actually a blueshift drift) in this model. The result is depicted in Fig. 4 where we have plotted the blueshift as a negative redshift. For this calculation, we have set the proper time elapse δt_0 to the value of 10 years, i.e., 10^{-8} Gyr. This is the reason why the redshift drift is given in units Gyr^{-1}. We see from Fig. 4 that the redshift drift is negative and that its effect is very small, of order years^{-13} at a blueshift of around 0.7. Of course, since the model is already ruled out by the blueshift,

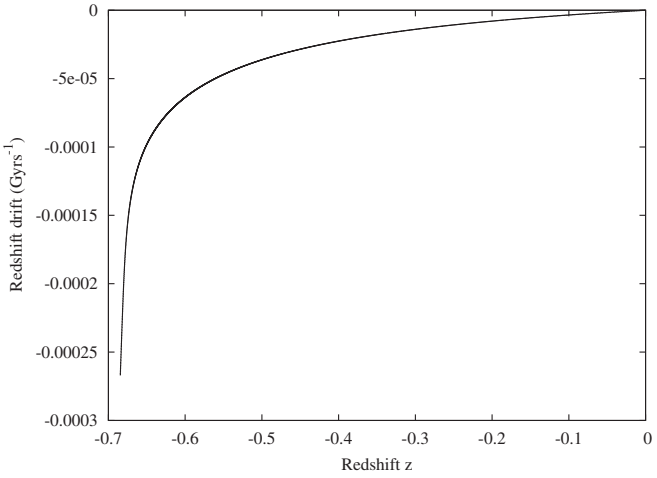

FIG. 4. The redshift drift (blueshift drift) as a function of the negative redshift (blueshift) z for the BSQSS model.

we do not need to worry about measuring such a small drift, but this computation shows that our recipe and our code for calculating the redshift drift work well and can be used for other general Szekeres models with no symmetry.

V. AVERAGING EFFECT: THE REDSHIFT AND THE REDSHIFT DRIFT IN THE MV MODEL

It has been shown in Ref. [20] that, once spatially averaged, the BSQSS model reproduces qualitatively the density profile of the LTB MV model of Ref. [21] with a central observer. We calculate in this section the MV model redshift to see what becomes of the BSQSS blueshift once the model is averaged. We find this blueshift becomes a cosmological redshift and then, to discriminate it from the ΛCDM model, we compute the MV model redshift drift.

A. LTB models

LTB models are spatially spherically symmetric solutions of Einstein's equations with dust as a gravitational source. Their metric in comoving and synchronous time gauge is, with the usual notations [45],

$$\mathrm{d}s^2 = -c^2\mathrm{d}t^2 + \frac{R'^2}{1+2E(r)}\mathrm{d}r^2 + R^2(t,r)(\mathrm{d}\theta^2 + \sin^2\theta\mathrm{d}\phi^2), \tag{5.1}$$

where $E(r)$ is an arbitrary function [corresponding to $-k(r)/2$ in QSS models and to $\bar{M}r^2k(r)$ in the MV model] and $R(t,r)$ obeys the same Eq. (2.4) as $\Phi(t,r)$ in QSS models, in which a new arbitrary function of r, $M(r)$, appears. A third arbitrary function, the $t_B(r)$ bang time, appears as an integration constant of (2.4) in (2.6). Hence, an LTB solution can be defined by three arbitrary functions of r, $E(r)$, $M(r)$, and $t_B(r)$.

The mass density in energy units is

$$\kappa\rho = \frac{2M'}{R'R^2}, \tag{5.2}$$

with $\kappa = 8\pi G/c^4$.

In the MV model, the cosmological constant Λ is also set to zero, since the aim is to reproduce the cosmological observations without dark energy. Then, the solutions to (2.4) are the same as (3.38)–(3.42), with an inverse sign for E as regards the one for k in the QSS models.

B. The equation for the redshift drift

After averaging the BSQSS model, the current observer is located at the center of the occurring LTB model [20]. Therefore, we give below the redshift drift equation for a central observer.

We consider a comoving observer O located at the origin, with coordinates $(t_0, r=0)$. The observer receives the light emitted by a comoving source at (t,r). We denote this source redshift by $z(t,r)$. After a δt_0 proper time elapse, the comoving observer moves to a new location, O' $(t_0+\delta t_0, r=0)$, and the comoving source moves to the new coordinates $(t+\delta t, r)$. Now, this source redshift observed at O' will be

$$Z(r) = z(r) + \delta z(r), \tag{5.3}$$

and its time coordinate

$$T(r) = t(r) + \delta t(r), \tag{5.4}$$

with $t(r=0)=t_0$, $z(r=0)=Z(r=0)=0$, $\delta z(r=0)=0$, and $\delta t(r=0)=\delta t_0$.

The equation for the redshift is

$$\frac{\mathrm{d}z}{\mathrm{d}r} = \frac{1+z}{c}\frac{\dot{R}'}{\sqrt{1+2E}}. \tag{5.5}$$

Differentiating (5.3) with respect to r and rearranging the terms, it comes to

$$\frac{\mathrm{d}\delta z(r)}{\mathrm{d}r} = \frac{\mathrm{d}Z(r)}{\mathrm{d}r} - \frac{\mathrm{d}z(r)}{\mathrm{d}r}. \tag{5.6}$$

Using (5.5) in (5.6) and keeping only the first order terms in δz and δt since they are very small compared to z and t, we obtain

$$\frac{\mathrm{d}\delta z}{\mathrm{d}r} = \frac{1+z}{c}\frac{\ddot{R}'(t,r)}{\sqrt{1+2E}}\delta t + \frac{\dot{R}'(t,r)}{\sqrt{1+2E}}\frac{\delta z}{c}. \tag{5.7}$$

Differentiating (5.4) with respect to r and rearranging the terms, it comes as

$$\frac{\mathrm{d}\delta t(r)}{\mathrm{d}r} = \frac{\mathrm{d}T(r)}{\mathrm{d}r} - \frac{\mathrm{d}t(r)}{\mathrm{d}r}. \tag{5.8}$$

Using the null condition equation, with the minus sign for incoming light rays, in (5.8) and keeping only the first order term in δt, we obtain

$$\frac{\mathrm{d}\delta t(r)}{\mathrm{d}r} = -\frac{1}{c}\frac{\dot{R}'(t,r)}{\sqrt{1+2E}}\delta t. \tag{5.9}$$

We consider the case where the redshift z is monotonically increasing with r. We replace the independent variable r by z by using the following chain rule of differentiation:

$$\frac{\mathrm{d}}{\mathrm{d}r} = \frac{\mathrm{d}z}{\mathrm{d}r}\frac{\mathrm{d}}{\mathrm{d}z} = \frac{1+z}{c}\frac{\dot{R}'}{\sqrt{1+2E}}\frac{\mathrm{d}}{\mathrm{d}z}. \tag{5.10}$$

Using (5.10) in (5.7) and rearranging the terms, we obtain

$$\frac{\mathrm{d}\delta z}{\mathrm{d}z} = \frac{\ddot{R}'}{\dot{R}'}\delta t + \frac{\delta z}{1+z}. \tag{5.11}$$

Similarly, using the transformation equation (5.10) in (5.9) and rearranging the terms, we obtain

$$\frac{\mathrm{d}\delta t}{\mathrm{d}z} = -\frac{\delta t}{1+z}. \tag{5.12}$$

We integrate (5.12) from the observer O at $(t_0, z=0)$ to the source at (t,z) and obtain

$$\delta t = \frac{\delta t_0}{1+z}. \tag{5.13}$$

We insert this expression for δt into (5.11) and obtain the equation for the redshift drift:

$$\frac{\mathrm{d}}{\mathrm{d}z}\left(\frac{\delta z}{1+z}\right) = \frac{1}{(1+z)^2}\frac{\ddot{R}'}{\dot{R}'}\delta t_0. \tag{5.14}$$

We numerically integrate (5.14) for a fixed δt_0 value to obtain δz, and then we calculate the redshift drift from its definition $\dot{z} = \delta z/\delta t_0$.

C. The minimum void model

This minimum void model is a void, in an Einstein-de Sitter (EdS) background, with minimal underdensity contrast around -0.4, and minimal radius of order 200–250 Mpc$/h$ able to reproduce the SN Ia data with no dark energy and to be consistent with the three-year WMAP data and measurements of the local Hubble parameter H_0.

In this LTB void model the mass function, the curvature function, and the bang time function are defined as follows, in units $c = G = 1$ and the Planck mass obeying $M_p^2 = 8\pi$:

$$M(r) = \frac{1}{6}\bar{M}^2 M_p^2 r^3, \tag{5.15}$$

$$E(r) = (\bar{M}r)^2 k_{\max}\left[1 - \left(\frac{r}{L}\right)^4\right]^2, \tag{5.16}$$

$$t_B(r) = 0, \tag{5.17}$$

where $\bar{M}$, $k_{\max}$, and L are parameters of the model and $E(r)$ is positive or null.

The $\bar{M}$ parameter is an arbitrary unphysical mass scale, related to the Hubble parameter via the following relation:

$$\bar{M} = \sqrt{\frac{3}{8\pi}}\frac{h_{\text{out}}}{3000}, \tag{5.18}$$

where h_{out} is the Hubble parameter in the EdS region.

One can see from (5.16) that the $k_{\max}$ parameter corresponds to the amplitude of the density fluctuation inside the void and L is the void radius beyond which the universe is described by a flat EdS metric.

For this model best fit to the data, the parameter values are $h_{\text{out}} = 0.452$, $k_{\max} = 5.302$, and L is 250 Mpc$/h$ where $h = 0.55$.

D. The algorithm for the MV model

In our numerical calculations, we use units in which the fundamental constants are set to their usual values. Notice that the factor of $1/3000$ in (5.18) appears for a $1/c$ factor. In order to calculate the redshift and the redshift drift, we proceed as follows:

(1) First, we compute $t(r)$ on the past light cone by numerically solving the following null condition equation for incoming geodesics in LTB models:

$$\frac{\mathrm{d}t}{\mathrm{d}r} = -\frac{1}{c}\frac{R'}{\sqrt{1+2E}}. \tag{5.19}$$

(2) Since $E(r)$, corresponding to the quantity we denoted $-k(r)/2$ in QSS models, is nearly everywhere positive, we use the parametric solution for QSS $k(r)$ negative. Substituting $t(r)$ in (3.42) we obtain $\eta(r)$, using which in (3.41) we calculate $R(t(r),r)$ and its derivatives on the past light cone.[1]

[1]The parametric equations are the same for QSS and LTB models because (2.4) with a vanishing Λ is the same.

(3) Then we numerically solve the following equation for the redshift $z(t(r), r)$:

$$\frac{\mathrm{d}z}{\mathrm{d}r} = \frac{1+z}{c}\frac{\dot{R}'}{\sqrt{1+2E}}. \tag{5.20}$$

(4) After having found z, we compute the redshift drift at this z by numerically solving (5.14).

E. The results

Figure 5 shows the redshift in the MV model up to the border of the void where $r = L = 450$ Mpc and $z = 0.085$. It is quite proportionally increasing with r up to around 300 Mpc above which the rate of increase slows down. This might be due to a nonproper matching between the void and the background EdS universe.

Figure 6 depicts the redshift drift behavior as a function of the redshift in the MV LTB model and in the ΛCDM model. In the redshift range of interest, the redshift drift in this LTB model remains negative while in the ΛCDM model it is positive. In principle, this may allow us to discriminate between both models even if they reproduce the same observational data. Also, in both models, the magnitude of the redshift drift increases monotonically with the redshift. However, it is a very small effect, of order Tyr^{-1} at the void border in the MV model, and therefore, very difficult to observe in future experiments.

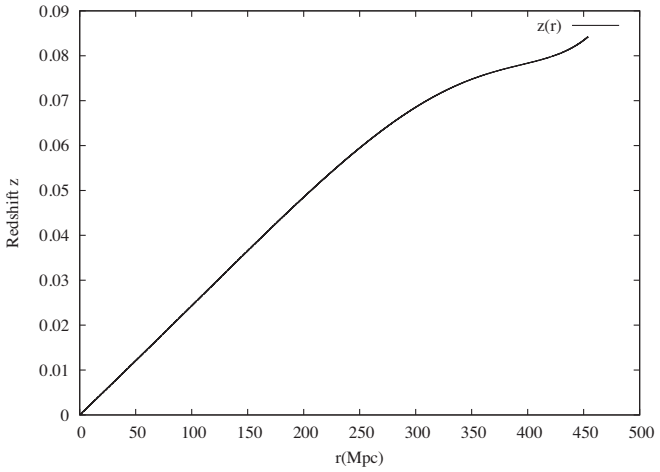

FIG. 5. The redshift (z) as a function of the comoving radial coordinate r for the MV model.

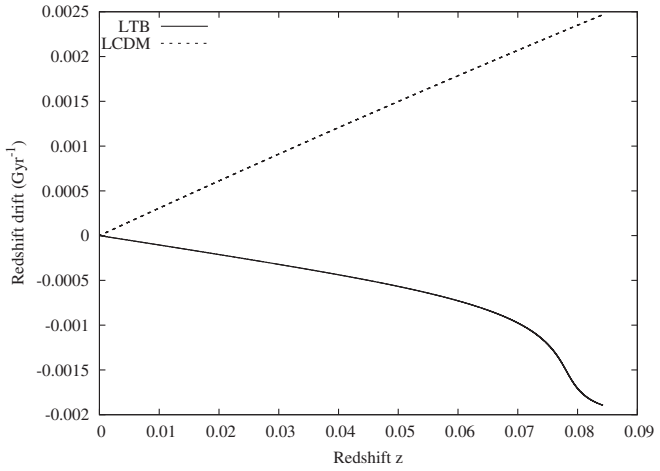

FIG. 6. The redshift drift ($\delta z/\delta t_0$) as a function of the redshift z for the MV model and the ΛCDM model.

VI. CONCLUSIONS

The type Ia supernova data, when analyzed in a FLRW framework, seems to be revealing that our universe expansion is accelerating from redshifts that correspond to nonlinear structure formation. In the standard ΛCDM cosmological model, this is put down to the effect of a dark energy component which, up to now, is not understood. Among different other explanations, the use of exact inhomogeneous models with no dark energy to reproduce the cosmological data has been rather extended in the literature. The first models used have been of the LTB class. These are dust spherically symmetric models and have been used either to build one patch models or to construct Swiss-cheese models (see, e.g., Refs. [15,46] for a review). However, we observe that the structures in the universe are not spherically symmetric. Therefore, $\Lambda = 0$ Szekeres models with no symmetry are now coming into play (see, e.g., [15,16,20,24,25]), the ones most frequently used being of the quasispherical class [45].

Now, these Szekeres models are much more complicated to deal with and the first authors who used them as cosmological models added some symmetry, e.g., axial [24,25]. Then, other studies have been made with Szekeres models with no symmetries [20,47]. However, it is very tricky to reproduce directly cosmological data with such models.

This is the reason why, in Ref. [20], the authors have considered a very general quasispherical Szekeres model, then spatially averaged it, and obtained the LTB MV model density profile of Ref. [21]. Since this MV model reproduces the SN Ia data and is consistent with the three-year WMAP data and the local Hubble parameter measurements, the Szekeres model of Ref. [20] can be considered as a proper inhomogeneous model which, once coarse grained and averaged, is consistent with these datasets. This strengthens the argument proposed in Ref. [48] that void model spherical symmetry is but a mathematical simplification of an energy density smoothed out over angles around us.

Now, models which reproduce the same cosmological data as ΛCDM ones on the observer past light cone cannot be distinguished from this model. The problem is completely degenerate. This is the reason why we have been interested in calculating the redshift drift of both models with a view to comparing them, first between them, then to

that of the ΛCDM model. We have therefore, for the first time in the literature to our knowledge, given two equation sets and an algorithm to compute the redshift drift in the most general QSS model. Then, we have applied them to the BSQSS model of Ref. [20]. One of the steps to obtain the redshift drift is to calculate the redshift and, in doing this for the BSQSS model, we have found that this redshift was negative, i.e., a blueshift. We observe this blueshift because the observer's location is not at the origin in this model. Actually, the origin is at the last scattering surface. Since, in this model, the universe is expanding away from this origin, the sources are coming toward the observer which is at $t = t_0$ and $r_0 = 100$ Mpc. Hence, the light rays are blueshifted. Since such a cosmological blueshift is not observed in the universe, this means that the nonaveraged BSQSS model is ruled out as a cosmological model. However, we cannot claim it is a generic feature of all quasispherical Szekeres models.

For completeness, and to test our recipe and our code, we have calculated the redshift drift (blueshift drift) for the BSQSS model. We have found that this redshift drift is negative, that its amplitude is increasing with the blueshift and that it is a very tiny effect. Indeed, for a ten-year observation, and around a blueshift of $z = -0.7$, the blueshift variation amplitude is $|\delta z| \sim 10^{-12}$. However, since the model is already ruled out by its blueshift, the redshift drift consideration is purely theoretical.

It has been shown in Ref. [20] that, once spatially averaged, the BSQSS model reproduces qualitatively the density profile of the LTB MV model of Ref. [21] with a central observer. We have thus calculated the MV model redshift to see what becomes of the BSQSS blueshift once the model is averaged. We have found that this blueshift becomes a cosmological redshift and then, to discriminate it from the ΛCDM model, we have computed the MV model redshift drift. This redshift appeared to be negative, with an amplitude increasing with redshift. On the contrary, in the redshift range of interest, the ΛCDM model redshift drift is positive which, in principle, would allow one to discriminate between both models by measuring their drift. However, these redshift drifts are also very tiny effects, since the void border is only at a small redshift of $z \sim 0.085$. At this redshift, the redshift variation amplitude of the MV model, for a ten-year observation, is merely $|\delta z| \sim 2.10^{-11}$. This will not be measurable by the future experiments dedicated to the redshift drift measurement in the universe such as CODEX/EXPRESSO [30,49,50], SKA [51], and the gravitational waves observations DECIGO/BBO [52].

However, the model proposed in Ref. [20] is a mere toy model, only reproducing a single void in a FLRW background. The important results of our paper are to show that, even if a QSS model of this kind exhibits a cosmological blueshift, the averaging process transforms it into a cosmological redshift which is in accordance with observations and that the redshift drift can, in principle, allow us to discriminate between the averaged model and the ΛCDM model while both reproduce the same cosmological data on the observer's past light cone.

It might happen that, in the future, more elaborate inhomogeneous models with no dark energy, such as Swiss-cheese models where the patches could be QSS without any symmetry and whose average might be LTB Swiss-cheeses reproducing the cosmological data, or QSS Swiss-cheese models reproducing themselves the data, should be proposed in the literature. In this case, our work could serve as a recipe to calculate the redshift and a then measurable redshift drift in these models. It has indeed been shown in Ref. [50] that a 42-m telescope is able to unambiguously detect the redshift drift over a 20-year period at a redshift $2 < z < 5$. Therefore, if one constructs a QSS Swiss-cheese model of the kind described above reaching a redshift of at least $z = 2$, the comparison with measured redshift drifts might become possible in the future.

[1] A. G. Riess, A. V. Filippenko, P. Chalis *et al.*, Astron. J. **116**, 1009 (1998).
[2] S. Perlmutter, G. Aldering, G. Goldhaber *et al.*, Astrophys. J. **517**, 565 (1999).
[3] A. N. Tawfik and E. A. El Dahab, Gravitation Cosmol. **25**, 103 (2019).
[4] T. Buchert, A. A. Coley, H. Kleinert, B. F. Roukema, and D. L. Wiltshire, Int. J. Mod. Phys. D **25**, 1630007 (2016).
[5] M. Cautun and C. S. Frenk, Mon. Not. R. Astron. Soc.: Lett. **468**, L41 (2017).
[6] A. Fuzfa and J.-M. Alimi, Phys. Rev. D **73**, 023520 (2006).
[7] P. Mishra and T. P. Singh, Int. J. Mod. Phys. A **21**, 1242002 (2012).
[8] J. W. Moffat, J. Cosmol. Astropart. Phys. 03 (2006) 004.
[9] T. Clifton, P. G. Ferreira, A. Padilla, and C. Skordis, Phys. Rep. **513**, 1 (2012).
[10] G. Lemaître, Ann. Soc. Sci. Bruxelles A **53**, 51 (1933); English translation, with historical comments: Gen. Relativ. Gravit. **29**, 641 (1997).
[11] R. C. Tolman, Proc. Natl. Acad. Sci. U.S.A. **20**, 169 (1934).
[12] H. Bondi, Mon. Not. R. Astron. Soc. **107**, 410 (1947).
[13] P. Szekeres, Commun. Math. Phys. **41**, 55 (1975).
[14] W. B. Bonnor, Commun. Math. Phys. **51**, 191 (1976).
[15] K. Bolejko, M.-N. Célérier, and A. Krasiński, Classical Quant. Grav. **28**, 164002 (2011).

[16] A. Nwanko, M. Ishak, and J. Thompson, J. Cosmol. Astropart. Phys. 05 (2011) 028.
[17] K. Bolejko and M. Korzyński, Int. J. Mod. Phys. D **26**, 1730011 (2017).
[18] K. Bolejko, J. Cosmol. Astropart. Phys. 06 (2017) 025.
[19] Z.-S. Zhang, T.-J. Zhang, H. Wang, and C. Ma, Phys. Rev. D **91**, 063506 (2015).
[20] K. Bolejko and R. Sussman, Phys. Lett. B **697**, 265 (2011).
[21] S. Alexander, T. Biswas, A. Notari, and D. Vaid, J. Cosmol. Astropart. Phys. 09 (2009) 025.
[22] A. Sandage, Astrophys. J. **136**, 319 (1962).
[23] G. McVittie, Astrophys. J. **136**, 334 (1962).
[24] P. Mishra, M.-N. Célérier, and T. P. Singh, Phys. Rev. D **86**, 083520 (2012).
[25] K. Bolejko and M.-N. Célérier, Phys. Rev. D **82**, 103510 (2010).
[26] J. Plebański and A. Krasiński, *An Introduction to General Relativity and Cosmology* (Cambridge University Press, Cambridge, England, 2006).
[27] V. A. Ruban, Pis'ma v Red. Zh. **8**, 669 (1968) [Sov. Phys. JETP Lett. **8**, 414 (1968)]; reprinted, with historical comments: Gen. Relativ. Gravit. **33**, 363 (2001).
[28] V. A. Ruban, Zh. Eksp. Teor. Fiz. **56**, 1914 (1969) [Sov. Phys. JETP **29**, 1027 (1969)]; reprinted, with historical comments: Gen. Relativ. Gravit. **33**, 375 (2001).
[29] C. Hellaby, Classical Quant. Grav. **13**, 2537 (1996).
[30] M. Quartin and L. Amendola, Phys. Rev. D **81**, 043522 (2010).
[31] C. M. Yoo, T. Kai, and K-i Nakao, Phys. Rev. D **83**, 043527 (2011).
[32] A. Balcerzak and M. P. Dabrowski, Phys. Rev. D **87**, 063506 (2013).
[33] A. Balcerzak and M. P. Dabrowski, Phys. Lett. B **728**, 15 (2014).
[34] J.-J. Geng, Y.-H. Li, J.-F. Zhang, and X. Zhang, Eur. Phys. J. C **75**, 356 (2015).
[35] J.-J. Geng, R.-Y. Guo, D.-Z. He, J.-F. Zhang, and X. Zhang, Front. Phys. **10**, 109501 (2015).
[36] S. M. Koksbang and S. Hannestad, J. Cosmol. Astropart. Phys. 01 (2016) 009.
[37] R.-Y. Guo and X. Zhang, Eur. Phys. J. C **76**, 163 (2016).
[38] M.-J. Zhang, H. Li, and J.-Q. Xia, Eur. Phys. J. C **77**, 434 (2017).
[39] E. G. Chirinos Isidro, C. Z. Vargas, and W. Zimdahl, J. Cosmol. Astropart. Phys. 05 (2016) 003.
[40] C. J. A. P. Martins, M. Martinelli, E. Calabrese, and M. P. L. P. Ramos, Phys. Rev. D **94**, 043001 (2016).
[41] A. Marconi *et al.*, Proc. SPIE Int. Soc. Opt. Eng. **9908**, 990823 (2016).
[42] D.-Z. He, J.-F. Zhang, and X. Zhang, Sci. China-Phys. Mech. Astron. **60**, 039511 (2017).
[43] F. Melia, Mon. Not. R. Astron. Soc.: Lett. **463**, L61 (2016).
[44] O. F. Piattella and L. Giani, Phys. Rev. D **95**, 101301 (2017).
[45] K. Bolejko, A. Krasiński, C. Hellaby, and M.-N. Célérier, *Structures in the Universe by Exact Methods—Formation, Evolution, Interactions* (Cambridge University Press, New York, 2010).
[46] V. Marra and A. Notari, Classical Quant. Grav. **28**, 164004 (2011).
[47] M. Ishak, A. Peel, and M. A. Troxel, Phys. Rev. Lett. **111**, 251302 (2013).
[48] M.-N. Célérier, Astron. Astrophys. **543**, A71 (2012).
[49] V. D'Odorico (for the CODEX/EXPRESSO team), Mem. Soc. Astron. Ital. **78**, 712 (2007).
[50] J. Liske, A. Grazian, E. Vanzella, M. Dessauges *et al.*, Mon. Not. R. Astron. Soc. **386**, 1192 (2008).
[51] H.-R. Klöckner, D. Obreschkow, C. Martins, A. Raccanelli, D. Champion, A. Roy, A. Lobanov, J. Wagner, and R. Keller, Real time cosmology—A direct measure of the expansion rate of the Universe, 'SKA Cosmology Chapter, Advancing Astrophysics with the SKA (AASKA14), Conference, Giardini Naxos (Italy), 2014.
[52] K. Yagi, A. Nishizawa, and C.-M. Yoo, J. Phys. Conf. Ser. **363**, 012056 (2012).